A Section 508–conformant HTML version of this article is available at https://doi.org/10.1289/EHP4949.

Environmental Electrophile-Mediated Toxicity in Mice Lacking Nrf2, CSE, or Both

Masahiro Akiyama,[1] Takamitsu Unoki,[1,2]* Yasuhiro Shinkai,[1]* Isao Ishii,[3] Tomoaki Ida,[4] Takaaki Akaike,[4] Masayuki Yamamoto,[5] and Yoshito Kumagai[1]*

[1]Environmental Biology Laboratory, Faculty of Medicine, University of Tsukuba, Tsukuba, Japan
[2]Department of Basic Medical Sciences, National Institute for Minamata Disease, Minamata, Japan
[3]Laboratory of Health Chemistry, Showa Pharmaceutical University, Tokyo, Japan
[4]Department of Environmental Health Sciences and Molecular Toxicology, Tohoku University Graduate School of Medicine, Sendai, Japan
[5]Department of Medical Biochemistry, Tohoku University Graduate School of Medicine, Sendai, Japan

Background: Transcription factor Nrf2 (nuclear factor-erythroid 2-related factor 2) plays a key role in detoxification of electrophiles via formation of glutathione (GSH) adducts and subsequent excretion into extracellular spaces. We found that reactive sulfur species (RSS), such as cysteine persulfides produced by cystathionine γ-lyase (CSE), capture environmental electrophiles through formation of sulfur adducts. However, contributions of Nrf2 and CSE to the blockage of environmental electrophile-mediated toxicity remain to be evaluated.

Objectives: The aim of this study was to clarify roles that CSE and Nrf2 play in the protection against various environmental electrophiles. We also wished to clarify the molecular basis of the developmental window of toxicity through investigating expression levels of Nrf2, RSS-producing enzymes, and sulfur nucleophiles during developmental stages of mice.

Methods: Wild-type (WT), CSE knockout (KO), Nrf2 KO, Nrf2/CSE double KO (DKO) mice, and their primary hepatocytes were analyzed in this study. Cadmium (Cd), methylmercury (MeHg), 1,4-naphthoquinone, crotonaldehyde, and acrylamide were used. We conducted Western blotting, real-time polymerase chain reaction (PCR), 3-(4,5-dimethylthiazol-2-yl)-2,5-triphenyl tetrazolium bromide (MTT) assays, liquid chromatography–electrospray ionization–tandem mass spectrometry (LC-ESI-MS/MS) analysis, alanine transaminase (ALT) activity, histopathological analysis, and rotarod test.

Results: Primary hepatocytes from DKO mice were significantly more sensitive to the environmental electrophiles than each single KO counterpart. Both Nrf2 and CSE single KO mice were highly susceptible to Cd and MeHg, and such sensitivity was further exacerbated in the DKO mice. Lower-level expressions of CSE and sulfur nucleophiles than those in adult mice were observed in a window of developmental stage.

Conclusions: Our mouse model provided new insights into the response to environmental electrophiles; while Nrf2 is recognized as a key transcription factor for detoxification of environmental electrophiles, CSE is crucial factor to repress their toxicity in a parallel mode. In addition, the sensitivity of fetuses to MeHg appears to be, at least in part, associated with the restricted production of RSS due to low-level expression of CSE. https://doi.org/10.1289/EHP4949

Introduction

Humans are exposed to various environmental electrophiles on a daily basis through food, air, and lifestyle. Some examples are naphthoquinones produced by combustion of gasoline, crotonaldehyde in tobacco smoke, methylmercury (MeHg) accumulated in fish, cadmium (Cd) in rice, and acrylamide in baked foods. Once these electrophiles enter the body, they target nucleophilic centers in various proteins and nitrogen atoms in DNA and form electrophile adducts, thereby exerting deleterious effects (Jan et al. 2015; Kanda et al. 2014; Kumagai and Abiko 2017; Saeed et al. 2007; Sumi 2008). However, it has been found that chemical modification of sensor proteins with reactive thiols by environmental electrophiles at low doses results in activation of cellular signal transduction pathways to maintain cellular homeostasis (Abiko et al. 2017a; Kumagai and Abiko 2017), although exposure to the reactive species at high doses causes cell damage through nonselective and excess modification of proteins and DNA (Kanda et al. 2014; Kumagai et al. 2012; Sumi 2008; Unoki et al. 2016).

Conjugation reactions of electrophiles with glutathione (GSH), which lead to the formation of their GSH adducts, are thought to be a canonical detoxification pathway of such reactive chemicals (Ketterer et al. 1983) because electrophile–glutathione (SG) adducts are polar substances and are rapidly excreted into extracellular spaces through multidrug resistance–associated proteins (MRPs) (Delalande et al. 2010; Kumagai et al. 2013; Toyama et al. 2011). In this context, transcription factor Nrf2 (nuclear factor-erythroid 2-related factor 2) has been shown to play a critical role in coordinating the cellular defense system by initiating the transcription of many detoxification and antioxidative stress genes (Lu 2013), including glutamate cysteine ligase (GCL; the rate-limiting enzyme for GSH synthesis) to synthesize GSH derived from cysteine (CysSH) (Lu 2013), glutathione *S*-transferase (GST) to facilitate GSH adduct formation (Itoh et al. 1997), and MRPs to excrete electrophile–GSH adducts into extracellular spaces (Hayashi et al. 2003; Itoh et al. 1997). Deletion of Nrf2 has been shown to enhance cellular toxicity of environmental electrophiles, including 1,2-naphthoquinone (1,2-NQ) (Miura et al. 2011) and MeHg (Toyama et al. 2007) in primary mouse hepatocytes, and Cd (Shinkai et al. 2016) in bovine vascular endothelial cells. Furthermore, Nrf2 activation by chemopreventive agents, such as sulforaphane, was effective to reduce MeHg accumulation and toxicity in primary mouse hepatocytes (Toyama et al. 2011). In contrast, GSH depletion in mice (Naganuma et al. 1988) and *in vitro* using primary cell cultures of mouse cerebellar neurons and astrocytes (Kaur et al. 2006) or MRP inhibition in rat pheochromocytoma PC12 cell sublines (Miura and Clarkson 1993) increased MeHg accumulation and toxicity, suggesting that Nrf2 is essential for the repression of environmental electrophile-mediated toxicity through GSH adduct formation and their excretion from cells to extracellular spaces.

Cystathionine γ-lyase (CSE) is the final trans-sulfuration enzyme required for cysteine biosynthesis from cystathionine (Steegborn et al. 1999). CSE has also been shown to catalyze

*These authors contributed equally to this work.
Address correspondence to Yoshito Kumagai, Environmental Biology Laboratory, Faculty of Medicine, University of Tsukuba, 1-1-1 Tennodai, Tsukuba, Ibaraki 305-8575, Japan. Telephone: +81-29-853-3133. Email: yk-em-tu@md.tsukuba.ac.jp

Supplemental Material is available online (https://doi.org/10.1289/EHP4949).
The authors declare they have no actual or potential competing financial interests.
Received 24 December 2018; Revised 9 May 2019; Accepted 10 May 2019; Published 5 June 2019.

the production of CysSH persulfide (CysSSH) when cystine (CysSSCys) is used as a substrate (Ida et al. 2014). Recently, an *in vitro* (HEK293T cells) and *in vivo* (mouse model) study revealed that cysteinyl-tRNA synthetase 2 (CARS2) also catalyzed formation of CysSSH using CysSH as a substrate (Akaike et al. 2017). CysSSH is converted to other reactive sulfur species (RSS), such as GSH persulfide/polysulfide, hydrogen sulfide (H_2S), and hydrogen persulfide (H_2S_2) (Ida et al. 2014; Ono et al. 2014). RSS are highly nucleophilic and antioxidative molecules (Ida et al. 2014), because sulfane sulfur within such molecules easily reacts with electrophiles to form the corresponding sulfur adducts (Kumagai and Abiko 2017; Millikin et al. 2016; Nishida et al. 2016; Ono et al. 2014). For example, we identified sulfur adducts of environmental electrophiles such as bismethylmercury sulfide [$(MeHg)_2S$] (Yoshida et al. 2011), cadmium sulfide (Akiyama et al. 2017), and 2-[(1,4-dioxonaphthalen-2-yl)sulfanyl]-3-hydroxynaphthalene-1,4-dione (Abiko et al. 2017b) during incubation of reactive persulfide/polysulfide with MeHg, Cd, and 1,4-NQ (1,4-naphthoquinone), respectively. Such sulfur adducts are weak electrophiles and less toxic than their parent electrophiles (Abiko et al. 2015b, 2017b; Akiyama et al. 2017; Yoshida et al. 2011), suggesting that RSS derived from CSE are involved in the formation of inactive metabolites of environmental electrophiles.

Consistent with this notion, exposure of mice to MeHg resulted in production of $(MeHg)_2S$ in various tissues of wild-type (WT) but not CSE knockout (KO) mice (Abiko et al. 2015b), suggesting that CSE participates in diminishment of environmental electrophile-mediated toxicity through formation of sulfur adducts. Although we have reported that knockdown or deletion of CSE enhances Cd-mediated toxicity both *in vitro* (Shinkai et al. 2017) and *in vivo* (Akiyama et al. 2017), there remains to be clarified how the protective function of CSE operates against other environmental electrophile-mediated toxicities. In this study, therefore, we hypothesized that in addition to GSH adduct formation regulated by Nrf2, sulfur adduct formation regulated by CSE plays a critical role in protection against environmental electrophiles. To address this hypothesis, we have evaluated individual and concurrent contributions of Nrf2 and CSE to the suppression of environmental electrophile-induced toxicity using Nrf2 KO, CSE KO, and Nrf2/CSE double KO (DKO) mice. We also examined precise expression profiles of Nrf2, RSS-producing enzymes including CSE, and the levels of sulfur nucleophiles during developmental stages of mice to assess contributions of both pathways to the developmental toxicity of the environmental electrophiles.

Methods

Materials

Acrylamide and cadmium chloride ($CdCl_2$) were purchased from Wako Pure Chemical Industries. Crotonaldehyde, MeHg, and paraformaldehyde (PFA) were from Nacalai Tesque. L-Cysteine-$^{13}C_2$,^{15}N was from Taiyo Nissan. GSH-(glycine-$^{13}C_2$,^{15}N) was from Toronto Research Chemicals. Amicon® Ultra 3K centrifugal filters; 1,4-NQ; PD MiniTrap™ G-25; and β-(4-hydroxyphenyl)ethyl iodoacetamide (HPE-IAM) were from Millipore, Tokyo Chemical Industries, GE Healthcare, and Molecular Biosciences, respectively. All other reagents and chemicals were of the highest grades available.

Animals and Treatment

The experimental design of this study is shown in Figure 1. C57BL6/J (WT) mice were purchased from Nippon Clea. CSE KO mice (Ishii et al. 2010), Nrf2 KO mice (Itoh et al. 1997) on a C57BL/6J background were maintained at the animal facilities at University of Tsukuba. Nrf2 KO and CSE KO mice were bred to generate heterozygous Nrf2/CSE DKO mice. These heterozygous DKO mice were bred to each other to generate Nrf2/CSE DKO mice. These mice were housed in plastic cages and maintained in a climate-controlled animal room (temperature: 24 ± 1°C; humidity: $55\% \pm 5\%$) with a 12-h light–dark cycle (lights on at 0700 hours and off at 1900 hours). Food (Certified Diet M; Oriental Yeast) and water were freely available.

Genotypes were confirmed by polymerase chain reaction (PCR) using tail DNA and the following primers: primer 1, 5′-TGCCGACCAATAAGCAGGGC-3′; primer 2, 5′-CCGAGGACTGGCCCGGGAAGT-3′; and primer 3, 5′-CCAGACCGGCAACGAAAATCA-3′; for CSE KO, primer 1 5′-TGGACGGGACTATTGAAGGCTG-3′, primer 2, 5′-GCCGCCTTTTCAGTAGATGGAGG-3′, and primer 3, 5′-GCGGATTGACCGTAATGGGATAGG-3′ for Nrf2 KO. PCR conditions were as follows: 96°C for 10 min; 40 cycles of 96°C for 30 s, 59°C for 30 s, 72°C for 30 s, and then 72°C for 10 min. After genotyping, mice were divided by gender and genotype. Males were used for the *in vivo* Cd exposure experiment. Females were used for the *in vivo* MeHg exposure experiment or primary hepatocyte studies. Note: The gender of the mouse is not chosen based on a specific biological reason. The reason for dividing the mouse into male and female is to reduce the number of animal sacrifices.

$CdCl_2$ and MeHg were dissolved in saline and deionized water, respectively. These solutions were prepared at the time of use. Acute hepatotoxicity was induced in adult male WT, Nrf2 KO, CSE KO, and DKO mice ($n = 5$, each genotype) by a single intraperitoneal injection of $CdCl_2$ (4 mg/kg). Eighteen hours after treatment, mice were anesthetized with pentobarbital, and blood was collected with heparin via cardiac puncture, followed by perfusion with 4% PFA in phosphate-buffered saline (PBS). Plasma was isolated from blood by centrifugation at $800 \times g$ at 4°C for 20 min. Fresh plasma was used for alanine transaminase (ALT) assays. Liver tissues were dissected and fixed in 4% PFA in PBS at 4°C overnight. Fixed tissues were embedded in paraffin for histopathological analysis. Adult female WT, CSE KO, Nrf2 KO, and DKO mice ($n = 5$, each genotype) were exposed to MeHg (5 mg/kg once daily for 12 d) by oral intubation and then subjected to the rotarod test. Survival of mice were monitored daily for 30 d after the first treatment of MeHg. Untreated WT mice at embryonic day (E) 15.5, postnatal day (P) 0, P7, P14, and P56 ($n = 3$, each age) were sacrificed; livers and brains were removed and stored at −80°C for Western blotting analysis, sulfur nucleophile detection, CSE activity measurement, and real-time PCR. Animal housing, husbandry, treatment, and euthanasia were conducted under the guidelines of the Animal Care and Use Committee of the University of Tsukuba. Experimental protocols for mice were approved by the Animal Care and Use Committee of the University of Tsukuba.

Preparation of Primary Mouse Hepatocytes

Primary hepatocytes were isolated as described previously (Shinkai et al. 2009). Briefly, cells were isolated from adult female WT, CSE KO, Nrf2 KO, and DKO mice by two-step collagenase perfusion. Parenchymal hepatocytes were separated from nonparenchymal cells by differential centrifugation ($50 \times g$, 3 min, 4°C), resuspended in Percoll buffer [Hank's balanced salt solution (HBSS) with 42% Percoll, 0.25% bovine serum albumin fraction V, 20 mM [4-(2-hydroxyethyl)-1-piperazineethanesulfonic acid] (HEPES; pH 7.3)]. Living parenchymal cell pellet were separated from dead parenchymal cell layer by density gradient centrifugation ($50 \times g$, 3 min, 4°C) and subsequently washed in HBSS and recovered by centrifugation ($50 \times g$, 3 min, 4°C). Final preparations were suspended at

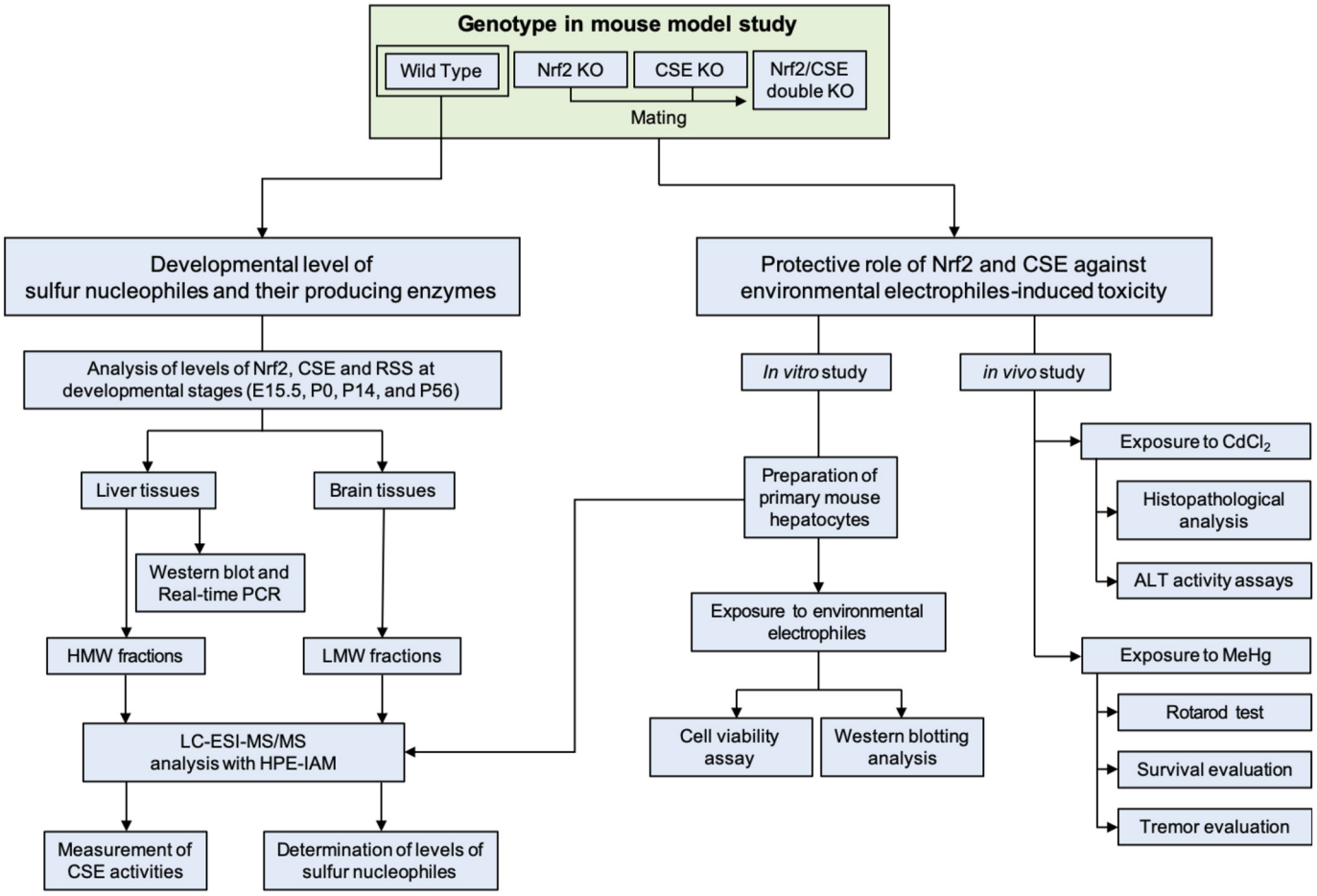

Figure 1. Flowchart of the experimental design. WT, CSE knockout (KO), Nrf2 KO, and DKO mice and their primary hepatocytes were used to clarify the protective role of Nrf2 and CSE against environmental electrophiles-induced toxicity (right side). The developmental stages of WT mice was used to analyze the developmental level of sulfur nucleophiles and its related enzymes (left side). Note: CSE, cystathionine γ-lyase; DKO, Nrf2/CSE double knockout; Nrf2, nuclear factor-erythroid 2-related factor 2; RSS, reactive sulfur species; WT, wild type.

4.0×10^5 cells/mL in William's Medium E containing 10% fetal bovine serum, 2 mM L-alanyl-L-glutamine, penicillin (100 units/mL), and streptomycin (100 μg/mL), then seeded at a density of 8×10^4 cells/cm^2 on 12- or 96-well type I collagen-coated plates (Corning Inc.), and cultured at 37°C in a humidified atmosphere with 5% CO_2. At 48 h after seeding, cells were cultured in serum-free medium for 24 h. These preparation steps were carried out independently three times from each genotype mice and used for assays employed such as Western blotting analysis, cell viability assay, and sulfur nucleophile detection, as described below.

Western Blotting Analysis

Primary mouse hepatocytes in 12-well plates prepared as above from adult female WT and CSE KO mice were exposed to $CdCl_2$ (0, 1, 2, or 4 μM) in serum-free medium and cultured at 37°C in a humidified atmosphere with 5% CO_2. After 12 or 24 h, cells were washed twice with ice-cold PBS. Total cellular protein samples were prepared by lysis of cells in sodium dodecyl sulfate (SDS) sample buffer (50 mM-Tris-HCl (pH 6.8), 2% SDS, and 10% glycerol), followed by incubation at 95°C for 10 min. Livers of untreated WT mice at E15.5, P0, P14, and P56 were sonicated in lysis buffer [50-mM Tris-HCl (pH 7.4), 1% Nonidet P-40, 0.1% sodium deoxycholate, 0.1% SDS, 150-mM NaCl, and 1% proteinase inhibitor cocktail (Cat # 03,969-21; Nacalai Tesque)]. The tissue lysates were centrifuged (9,000 × *g*, 10 min, 4°C) to remove insoluble material. Protein concentrations were determined using a bicinchoninic acid (BCA) protein assay reagent kit (Pierce Biotechnology) before 2-mercaptoethanol and bromophenol blue were added to each sample. The protein samples (15 μg/well) were separated by SDS–polyacrylamide gel electrophoresis and then electrotransferred onto a polyvinyl difluoride membrane (FluoreTrans®, PVM020C-099) (Bio-Rad Laboratories) at 2 mA/cm^2 for 1 h, as described previously (Kyhseandersen 1984). Membranes were blocked with 5% dry skim milk in Tris-buffered saline with detergent [20 mM Tris-HCl (pH 7.5), 150 mM NaCl, and 0.1% Tween 20] and then incubated with a primary antibody for 1 h at room temperature: an antihemeoxygenase-1 (HO-1) antibody (1:1,000; Cat #SPA-895; Lot #01,101,357; StressGen Biotechnologies), anti-Nrf2 antibody (1:200; Cat #sc-13,032; Lot #D0815; Santa Cruz Biotechnology), and anti-CSE antibody were prepared as described previously (20 μg/mL) (Shinkai et al. 2017). Immunoreactive bands were visualized by enhanced chemiluminescence (Chemi-Lumi One L; Nacalai Tesque) and detected with a LAS-3000 (Fujifilm). Signal intensities were quantified by Multi Gauge software, version 2.2 (Fujifilm).

Cell Viability Assay

The 3-(4,5-dimethylthiazol-2-yl)-2,5-triphenyl tetrazolium bromide (MTT) assay was used to estimate cell viability, as described previously (Denizot and Lang 1986). Briefly, primary mouse hepatocytes in 96-well plates prepared as above from WT, CSE

KO, Nrf2 KO, and DKO mice were exposed to environmental electrophiles ($CdCl_2$, MeHg, 1,4-NQ, crotonaldehyde, or acrylamide) in serum-free medium and cultured at 37°C in a humidified atmosphere with 5% CO_2. Nonexposed cells were used as control. After 24 h, cells were treated with 5 mg/mL MTT for 4 h at 37°C. After removing the medium, dimethylsulfoxide (100 μL/well) was added to dissolve the formazan precipitate. Absorbance at 540 nm was read with an iMark™ microplate reader (Bio-Rad Laboratories).

Sulfur Nucleophile Detection

Liquid chromatography–electrospray ionization–tandem mass spectrometry (LC-ESI-MS/MS) analysis with HPE-IAM was used to determine the levels of sulfur nucleophiles, including reactive persulfides, in primary mouse hepatocytes and brain tissue, as we previously established (Akaike et al. 2017). Primary mouse hepatocytes in 12-well plates prepared as above from WT, CSE KO, Nrf2 KO, and DKO mice were washed twice with ice-cold PBS and collected by scraping into PBS; then cellular pellets were recovered by centrifugation (500 × *g*, 5 min, 4°C). Using an ultrasonic disruptor, UD-201 (TOMY), cellular pellets were homogenized in 100 μL of a methanol solution containing 1 mM HPE-IAM on ice, after which cell lysates were incubated at 37°C for 30 min to yield β-(4-hydroxyphenyl)ethyl acetamide (HPE-AM) adducts of sulfur nucleophiles. After centrifugation (14,000 × *g*, 10 min, 4°C), supernatants were collected. Brain samples (100 mg each) of untreated WT mice at E15.5, P0, P14, and P56 were sonicated in 1-mL lysis buffer [50-mM Tris-HCl (pH 7.4), 1% Nonidet P-40, 0.1% sodium deoxycholate, 0.1% SDS, 150-mM NaCl, and 1% proteinase inhibitor cocktail]. The tissue lysates were centrifuged (9,000 × *g*, 10 min, 4°C) to remove insoluble material. The supernatants were filtered through an Amicon® Ultra 3K to obtain low-molecular-weight (LMW) fractions. The LMW fractions were incubated with 5-mM HPE-IAM at 37°C for 30 min to yield HPE-AM adducts of sulfur nucleophiles. Aliquots containing HPE-AM adducts were diluted fourfold with 0.1% formic acid containing known amounts of isotope-labeled internal standards (Table S1), which were then analyzed by LC-ESI-MS/MS for sulfur nucleophile determination. A triple quadrupole mass spectrometer, EVOQ Qube™ (Bruker), coupled to the Advance™ UHPLC system (Bruker) was used to perform LC-ESI-MS/MS. Sulfur nucleophile–derived HPE-AM adducts were separated by Advance™ UHPLC with a YMC-Triart C18 column (50 × 2.0 mm inner diameter) under the following elution conditions: mobile phase A (0.1% formic acid) with a linear gradient of mobile phase B (0.1% formic acid in methanol) from 5% to 90% for 15 min at a flow rate of 0.2 mL/min at 40°C. Mass spectra were obtained at each temperature of the ESI probe, desolvation line, and heat block at 350 and 250°C, respectively. The nebulizer, heating, and drying nitrogen gas flows were set to 25, 50, and 50 pound per square inch (psi), respectively. Various HPE-AM adducts of sulfur nucleophiles were identified and quantified by multiple reaction monitoring.

Alanine Transaminase Activity Assays

ALT assays were performed using the Transaminase C-II Test Wako kit (Wako Pure Chemical Industries), according to the manufacturers' instructions.

Histopathological Analysis

Paraffin-embedded liver tissue was sectioned to 3-μm-thick sections. Tissue sections were stained with hematoxylin and eosin (H&E) and Masson's trichrome (MT) by standard techniques. Images were acquired using a brightfield microscope, BZ-X710 (Keyence).

Mouse Behavioral Test

The rotarod test evaluates motor coordination, balance, and motor learning. The Rota-Rod, ENV-577M (Med Associates) was accelerated from 0 to 40 rpm over 4 min and maintained at a constant speed for an additional 1 min. The latency to fall was then recorded. Animals were subjected to daily sessions of three trials separated by 15-min intertrial intervals. The test was repeated for 16 consecutive days after the first day of exposure. The latency to fall was scored each time as an index of motor coordination. Percent of tremors were calculated as the number of mice that had at least one tremor divided by the total number of mice in each group. Tremors were monitored daily for 14 d after the first treatment of MeHg.

CSE Activity Measurement

Liver tissues of untreated WT mice at E15.5, P0, P14, and P56 were homogenized in 50 mM Tris-HCl (pH 7.5) containing the proteinase inhibitor cocktail, followed by centrifugation at 9,000 × *g* for 10 min at 4°C. The supernatants were applied to a PD MiniTrap™ G-25 column equilibrated with 50 mM Tris-HCl (pH 7.5) to obtain high-molecular-weight (HMW) fractions. The reaction mixture (100 μL) contained 100 mM HEPES buffer (pH 7.5), 0.5 mM cystathionine or CysSSCys, 0.1 mM pyridoxal phosphate, and protein (100 μg) from the HMW fraction. The reaction mixture was incubated at 37°C for 30 min and then deproteinized in methanol, followed by centrifugation at 14,000 × *g* for 10 min at 4°C. The supernatants were then subjected to LC-ESI-MS/MS analysis.

Real-Time Polymerase Chain Reaction

Total RNA from livers of untreated WT mice at E15.5, P0, P7, P14, and P56 were extracted with RNeasy Lipid Tissue Mini Kit (Qiagen), and cDNA was synthesized using High-Capacity cDNA Reverse Transcription Kit (Applied Biosystems™), according to the manufacturers' protocols. Real-time PCR was performed using Power SYBR™ Green PCR Master Mix (Applied Biosystems™) with a 7500 Real-Time PCR System (Applied Biosystems™). The PCR primers were designed as follows: forward 5′-CTTGCTGCC ACCATTACG-3′ and reverse 5′-TTCAGATGCCACCCTCCT-3′ for *Cse* (Li et al. 2015), forward 5′-CGAGATATACGCAGGAGA-GGTAAGA-3′ and reverse 5′-GCTCGACAATGTTCTCCAG-CTT-3′ for *Nrf2* (Jiang et al. 2016), forward 5′-GTCTTCCACCA-GTGTCAGCA-3′ and reverse 5′-GGTCTTCAGGAAGTCCTT-AATGGT-3′ for *Cars2* (design with Primer3Plus: http://www.bioinformatics.nl/cgi-bin/primer3plus/primer3plus.cgi/), and forward 5′-TCAACAGCAACTCCCACTCTTCCA-3′ and reverse 5′-ACCCTGTTGCTGTAGCCGTATTCA-3′ for glyceraldehyde 3-phosphate dehydrogenase (*Gapdh*) (Gnedeva and Hudspeth 2015). PCR conditions were 50°C for 2 min, 95°C for 10 min, and 45 cycles of 95°C for 15 s and 60°C for 1 min. Melting curve analysis was conducted to ensure amplification of a single product. *Cse*, *Nrf2*, *Cars2*, and *Gapdh* mRNA levels in each RNA sample were determined using a standard curve. Fold changes in expression of each gene were assessed after the mRNA level was normalized to *Gapdh* expression.

Statistical Analysis

Statistical significance was assessed by analysis of variance (ANOVA) with correction for multiple comparisons in post-hoc analysis. Rotarod test were analyzed by a two-way repeated-measures ANOVA with Dunnett's post hoc test. Other multiple comparisons were analyzed by one-way ANOVA with Dunnett's or Tukey's post hoc test. Survival rates were analyzed by Log-rank (Mantel-Cox) test. All statistical analyses were performed

using Graphpad Prism, version 6.0h (Graphpad Software). A $p < 0.05$ was considered as significant.

Results

Production of Sulfur Nucleophiles in Wild-Type, CSE Knockout, Nrf2 Knockout, and Double-Knockout Mouse Hepatocytes

We examined sulfur nucleophile levels in primary mouse hepatocytes from WT, CSE KO, Nrf2 KO, and DKO mice by means of LC-ESI-MS/MS analysis. We found that in the hepatocytes of CSE KO and DKO mice, GSH, CysSH, CysSSH, and GSSH levels were significantly lower compared with WT cells, whereas in Nrf2 KO mice hepatocytes, only the GSH level was significantly lower (Figure 2).

Roles of Nrf2 and CSE in Protection of Liver Cells against Environmental Electrophiles

We then exposed the primary hepatocytes from WT, CSE KO, Nrf2 KO, and DKO mice to various environmental electrophiles, including Cd; MeHg; 1,4-NQ; crotonaldehyde; and acrylamide, and assessed cytotoxicity of these environmental electrophiles. Their cytotoxicity were evaluated by median lethal concentration values (Table 1), which were determined from a dose-dependent cell viability curve using the MTT assay on the primary hepatocytes of each genotype treated with various environmental electrophiles (Figure 3A–E). As shown in Figure 3 and Table 1, Nrf2 deletion (triangle dots) resulted in significantly greater cell toxicity by Cd; MeHg; and 1,4-NQ, whereas CSE deletion (square dots) resulted in significantly greater Cd-mediated cytotoxicity only (Figure 3A–C). Neither Nrf2 nor CSE deletion caused significantly greater cytotoxicity by crotonaldehyde or acrylamide compared with WT mice (Figure 3D,E).

In contrast, the cytotoxicity of all examined environmental electrophiles was markedly greater in the DKO hepatocytes (diamond dots) than with the single-KO counterparts (Figure 3A–E). We also examined the effect of CSE deletion on Nrf2 induced by Cd because we found that level of all evaluated sulfur nucleophiles was lower in the CSE KO mice than in the WT mice (Figure 2). As a result, we found that CSE KO mice had significantly higher levels of Nrf2 and its downstream protein HO-1 after treatment with Cd (Figure 3F).

Treatment of WT mice with $CdCl_2$ (4 mg/kg) did not affect liver when evaluated by H&E and MT staining, whereas CSE KO or Nrf2 KO mice with the same dose of $CdCl_2$ injection showed liver damage as indicated by HE staining (Figure 3G, dotted lines). Cd-treated DKO mice exhibited much more severer liver injury and fibrosis than WT mice and CSE and Nrf2 single-KO mice (Figure 3G, blue stained area). Consistent with these results, the plasma ALT level, another indicator of hepatotoxicity, in DKO mice was much higher than that in CSE or Nrf2 single-KO mice treated with Cd (Figure 3H). Plasma ALT levels without the Cd treatment were not significantly different in all genotypes (Figure S1).

Contribution of CSE to Protection against MeHg-Induced Neurotoxicity

Under non–MeHg treated conditions, WT, CSE KO, Nrf2 KO, and DKO mice showed comparable motor coordination as measured by the rotarod test (Figure 4A), and no tremors (Figure 4B). However, MeHg treatment (5 mg/kg for 12 d) resulted in significantly poorer motor coordination and a greater number of detectable tremors in CSE KO, Nrf2 KO, and DKO mice, but not in WT mice (Figure 4A,B). Survival rates were also significantly lower for MeHg-treated CSE KO, Nrf2 KO, and DKO mice than for MeHg-treated WT mice (Figure 4C). All single-KO and DKO mice died within 21 and 14 d after the first treatment of MeHg, whereas WT mice given MeHg shown no mortality and were healthy appearing for at least 30 d after the first treatment of MeHg. The effects of MeHg on motor coordination and tremors appeared to be exacerbated in DKO mice compared with Nrf2 or CSE KO mice (Figure 4A,B), with the survival effects in the DKO mice appearing to be more severe than the sum of those in either KO alone (Figure 4C).

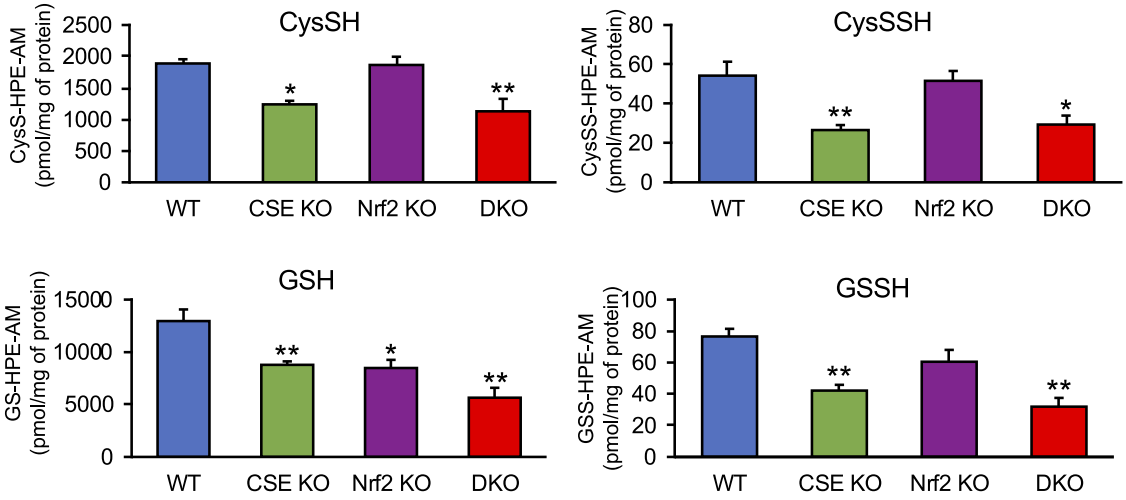

Figure 2. Effects of CSE and/or Nrf2 deletion on sulfur nucleophile contents. Sulfur nucleophile levels in primary mouse hepatocytes from WT, CSE knockout (KO), Nrf2 KO, and DKO female mice. Cells were sonicated and incubated with 1 mM β-(4-hydroxyphenyl)ethyl iodoacetamide (HPE-IAM) at 37°C for 30 min to yield HPE-AM adducts. The adducts were identified and quantified by liquid chromatography–electrospray ionization–tandem mass spectrometry (LC-ESI-MS/MS) using isotope-labeled internal standards. Data are shown as mean ± standard error of the mean (SEM) ($n = 3$, each genotype). Note: CSE, cystathionine γ-lyase; DKO, Nrf2/CSE double knockout; CysSH, cysteine; CysSSH, cysteine persulfide; GSH, glutathione; GSSH, glutathione persulfide; HPE-AM, β-(4-hydroxyphenyl)ethyl acetamide; Nrf2, nuclear factor-erythroid 2-related factor 2; WT, wild type. *$p < 0.05$ and **$p < 0.01$, compared with WT cells by one-way analysis of variance (ANOVA) with Tukey's post hoc test.

Table 1. Comparison of lethal doses in CSE and/or Nrf2-deficient primary mouse hepatocytes exposed to various environmental electrophiles.

	Cd		MeHg		1,4-NQ		Crotonaldehyde		Acrylamide	
	LC_{50} (μM)	95% confidence intervals	LC_{50} (μM)	95% confidence intervals	LC_{50} (μM)	95% confidence intervals	LC_{50} (μM)	95% confidence intervals	LC_{50} (μM)	95% confidence intervals
WT	16.8	15.4, 18.3	7.9	7.6, 8.3	5.2	5.0, 5.4	214	206, 223	19.4	16.5, 22.8
CSE KO	9.0^{a}	8.0, 10.0	9.1	8.6, 9.7	6.0	5.8, 6.2	200	193, 209	18.2	16.4, 20.2
Nrf2 KO	5.4^{a}	4.8, 6.0	3.5^{a}	3.4, 3.7	4.0^{a}	3.8, 4.2	231	222, 240	19.6	17.1, 22.5
DKO	$1.5^{a,b,c}$	1.3, 1.8	$1.5^{a,b,c}$	1.4, 1.7	$2.7^{a,b,c}$	2.4, 3.0	$58^{a,b,c}$	53, 64	$3.1^{a,b,c}$	2.8, 3.4

Note: WT, CSE knockout (KO), Nrf2 KO, and DKO cells were exposed to the indicated compounds for 24 h, and then MTT assays were performed as shown in Figure 2. LC_{50} values were determined by nonlinear regression. Statistical analyses were performed by Graphpad Prism software from three independent experiments. Cd, cadmium; CSE, cystathionine γ-lyase; DKO, Nrf2/CSE double knockout; MeHg, methylmercury; MTT, 3-(4,5-dimethylthiazol-2-yl)-2,5-triphenyl tetrazolium bromide; Nrf2, nuclear factor-erythroid 2-related factor 2; WT, wild type; 1,4-NQ, 1,4-naphthoquinone.
$^{a}p < 0.01$, $^{b}p < 0.01$, $^{c}p < 0.01$ compared with WT, CSE KO, and Nrf2 KO, respectively, by one-way ANOVA of $\log_{10}$-transformed LC_{50} values with Tukey's post hoc test.

Developmental Expression of CSE and Reactive Sulfur Species

We investigated developmental expression of Nrf2, CSE, and other RSS-producing enzymes such as CARS2 in the livers of WT mice at the following developmental stages: E15.5, P0, P14, and the adult stage (P56). Western blot and real-time PCR analyses revealed that protein (Figure 5A) and mRNA (Figure S2A) levels of CSE at developmental stages such as E15.5 and P0 were significantly lower than those at the adult stage, while practically no appreciable differences of Nrf2 and CARS2 mRNA were seen except for Nrf2 at P0 (Figure S2B,C). Furthermore, when CSE

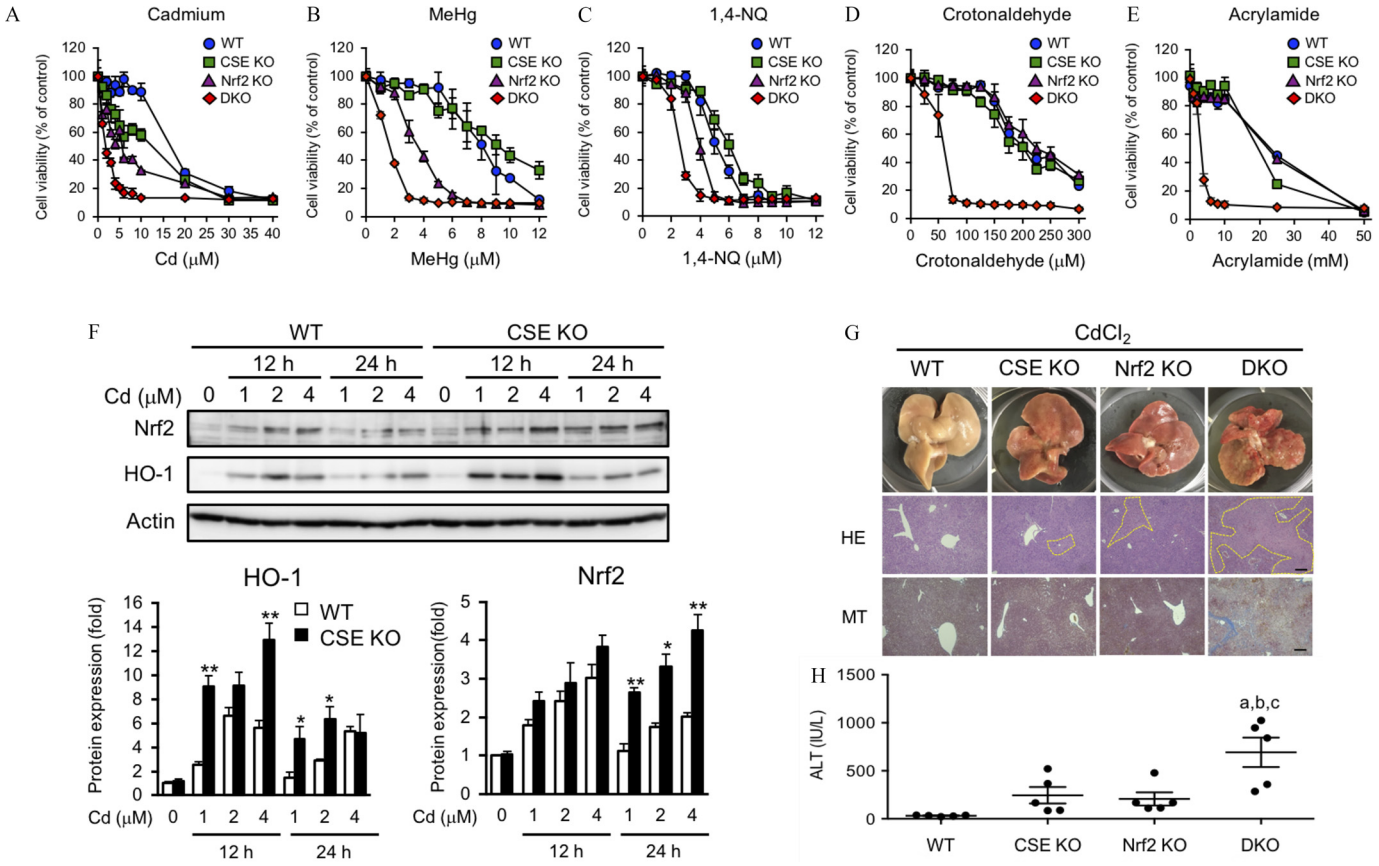

Figure 3. Effects of CSE and/or Nrf2 deletion on environmental electrophiles-induced hepatotoxicity *in vitro* and *in vivo*. (A–E) Primary hepatocytes from WT, CSE knockout (KO), Nrf2 KO, and DKO female mice were exposed to the indicated compounds at the indicated concentrations for 24 h, and then MTT assays were performed. Each value is the mean ± standard error of the mean (SEM) of three independent experiments. See also Table 1 for LC_{50} values with statistical analyses. (F) WT and CSE KO primary mouse hepatocytes were exposed to the indicated concentrations of $CdCl_2$ for 12 or 24 h. Total cell lysates (15 μg of protein) were subjected to Western blotting using the indicated antibodies. Representative images are shown. Actin was used to normalize protein levels. Intensities are presented as fold changes relative to 0 μM $CdCl_2$ exposure. Data are shown as mean ± SEM ($n = 3$, each genotype). $*p < 0.05$ and $**p < 0.01$, compared with 0 μM $CdCl_2$ exposure by one-way analysis of variance (ANOVA) with Tukey's post hoc test. (G–H) WT, CSE KO, Nrf2 KO, and DKO male mice were treated with or without $CdCl_2$. Liver tissue and plasma samples were collected after 18 h of treatment. (G) Representative stereoscopic images of liver from WT, CSE KO, Nrf2 KO, and DKO mice administered $CdCl_2$ (upper panels), corresponding hematoxylin and eosin (H&E)–stained liver sections (middle panels, necrotic area outlined), and Masson's trichrome (MT) staining of histopathological liver sections (bottom panels, blue staining indicates collagen fibers). (H) Plasma alanine transaminase (ALT) levels with $CdCl_2$ treatment. Scale bar represents 100 μm. Data are shown as mean ± SEM ($n = 5$, each genotype). $^{a}p < 0.05$, WT vs. DKO. $^{b}p < 0.05$, CSE KO vs. DKO. $^{c}p < 0.05$, Nrf2 KO vs. DKO. Statistical analysis was performed by one-way ANOVA with Tukey's post hoc test. Note: CSE, cystathionine γ-lyase; DKO, Nrf2/CSE double knockout; MTT, 3-(4,5-dimethylthiazol-2-yl)-2,5-triphenyl tetrazolium bromide; Nrf2, nuclear factor-erythroid 2-related factor 2; WT, wild type.

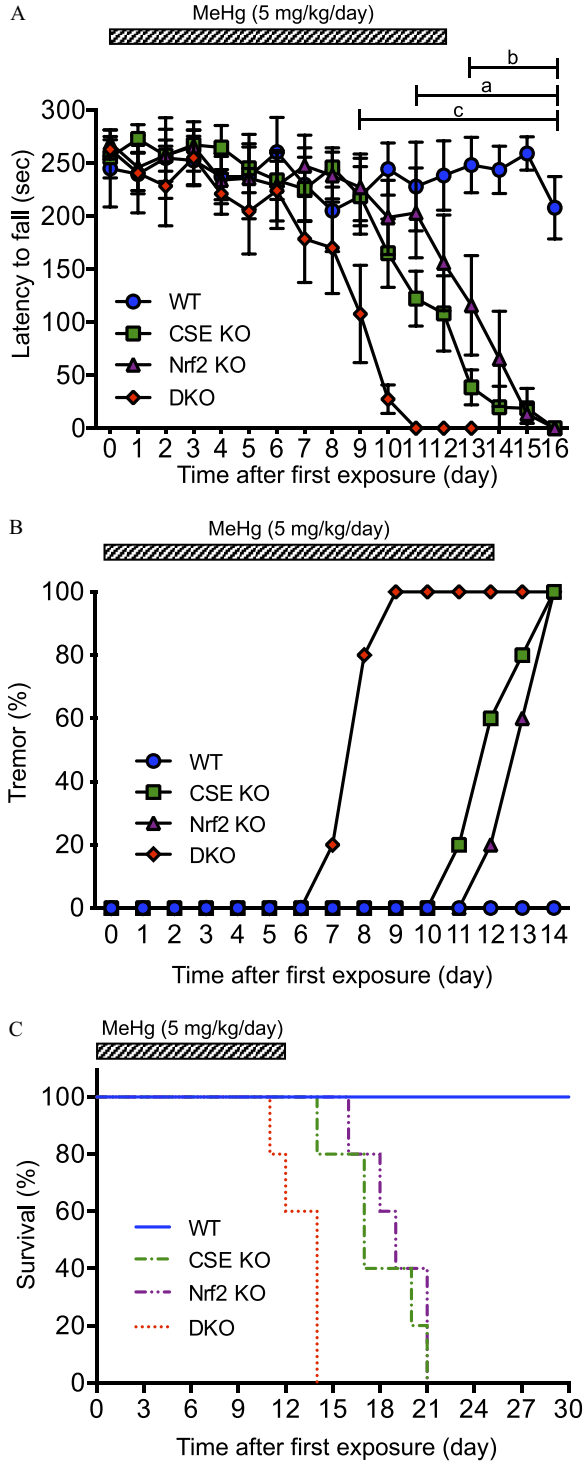

Figure 4. Effects of CSE and/or Nrf2 deletion on MeHg-induced neurotoxicity. (A–C) WT, CSE knockout (KO), Nrf2 KO, and DKO female mice were treated with MeHg (5 mg/kg/d) for 12 d. (A) Latency to fall during the rotarod test. The test was repeated for 16 consecutive days after the first day of exposure. Data are shown as mean ± standard error of the mean (SEM) ($n = 5$, each genotype). [a]$p < 0.05$, WT vs. CSE KO. [b]$p < 0.05$, WT vs. Nrf2 KO. [c]$p < 0.05$, WT vs. DKO. Rotarod test were analyzed by a two-way repeated-measures analysis of variance (ANOVA) with Dunnett's post hoc test to compare strains to the WT. (B) Percentage of total mice that had at least one tremor. Tremors were monitored daily for 14 d after the first treatment. (C) Survival rates for 30 d after the first treatment. Survival rates were analyzed by log-rank (Mantel-Cox) test. Note: CSE, cystathionine γ-lyase; DKO, Nrf2/CSE double knockout; Nrf2, nuclear factor-erythroid 2-related factor 2; WT, wild type.

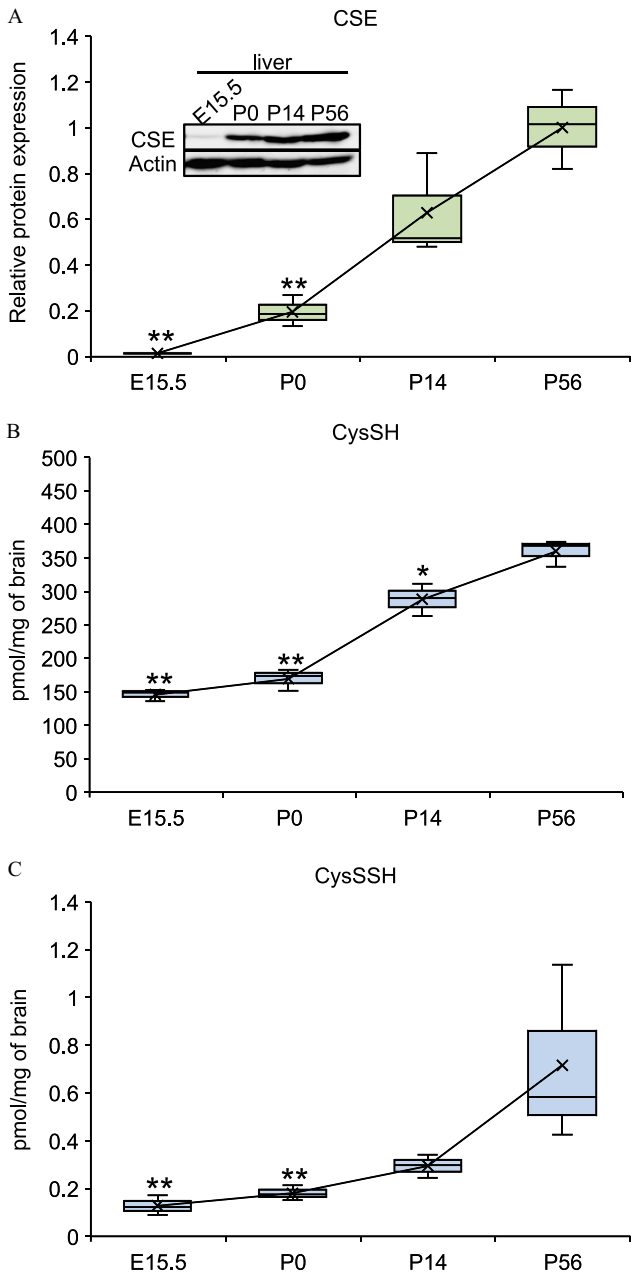

Figure 5. Developmental expression of hepatic CSE and levels of CysSH and its persulfide in the brain. (A) Liver tissues of WT mice at various developmental stages and the adult stage were analyzed for CSE protein expression by Western blotting. β-actin was used to normalize protein levels. (B–C) LC-ESI-MS/MS analysis was employed to determine the levels of (B) CysSH, and (C) CysSSH in low-molecular-weight fractions from the brains of mice at developmental and adult stages. Data are shown as box-and-whisker plot ($n = 3$, each age). The points, mean values; the horizontal lines, median values; the box limits, interquartile range; the whiskers, maximum and minimum data values. Note: CSE, cystathionine γ-lyase; CysSH, cysteine; CysSSH, cysteine persulfide; LC-ESI-MS/MS, liquid chromatography–electrospray ionization–tandem mass spectrometry; WT, wild type. *$p < 0.05$ and **$p < 0.01$, compared with the adult stage (P56) by one-way analysis of variance (ANOVA) with Dunnett's post hoc test.

activities involved in production of CysSH and its persulfide and polysulfide during developmental stages were measured after incubation of the mouse liver HMW fraction with cystathionine or CysSSCys as substrates, production of CysSH, CysSSH, and CysSH polysulfide (CysSSSH) at developmental stages was

Table 2. Product formation after incubation of liver proteins with CSE substrates.

Substrate	Product formed (μM)	Developmental stage			
		E15.5	P0	P14	P56
Cystathionine	CysSH	9.5 ± 0.4^b	110 ± 27^a	275 ± 62	332 ± 43
	CtysSSH	1.2 ± 0.2^b	5.4 ± 0.4^b	11.1 ± 0.5	12.7 ± 1.1
	CysSSSH	1.1 ± 0.1^b	1.5 ± 0.3^b	5.6 ± 0.5	6.2 ± 0.3
Cystine	CytsSH	134 ± 32	86 ± 25	85 ± 6	153 ± 18
	CysSSH	53 ± 2^b	68 ± 3^b	71 ± 2^b	85 ± 2
	CysSSSH	3.9 ± 0.3^b	10.2 ± 0.3^b	36.2 ± 2.3^b	93.9 ± 10.8

Note: Cystathionine (0.5 mM) or cystine (0.5 mM) were incubated with the high-molecular-weight fraction (1 mg/mL) from the liver of wild-type mice at various developmental stages and the adult stage in 100 mM HEPES buffer (pH 7.5) containing pyridoxal phosphate (0.1 mM) at 37°C for 30 min, and then CysSH, CysSSH, and CysSSSH were measured by β-(4-hydroxyphenyl)ethyl iodoacetamide labeling in liquid chromatography–electrospray ionization–tandem mass spectrometry (LC-ESI-MS/MS) analysis. Data are shown as mean ± standard error of the mean (SEM) ($n = 3$, each age). CSE, cystathionine γ-lyase; CysSH, cysteine; CysSSH, cysteine persulfide; CysSSSH, cysteine trisulfide; E, embryonic day; HEPES, [4-(2-hydroxyethyl)-1-piperazineethanesulfonic acid]; P, postnatal day.
$^a p < 0.05$ and $^b p < 0.01$, compared with the adult stage (P56) by one-way analysis of variance (ANOVA) with Dunnett's post hoc test.

lower than that at the adult stage when cystathionine was used (Table 2). In the case of CysSSCys, production of CysSSSH at developmental stages was lower than that at the adult stage. Consistent with these results, the levels of CysSH and CysSSH (Figure 5B,C), but not GSH or GSSH (Figure S3), in the brain at developmental stages were significantly lower than those at the adult stage.

Discussion

In this study, we found that both the Nrf2 pathway and CSE pathway play important roles in the protection against environmental electrophile-induced toxicity *in vitro* and *in vivo*. DKO mice were more sensitive to environmental electrophiles than their single-KO counterparts, suggesting that the pathways mediate different mechanisms in diminishing toxicities of reactive electrophiles (Figure 6). Nrf2-mediated defense mechanism against electrophiles is mainly attributable to GSH conjugation and its excretion into extracellular spaces (Hayashi et al. 2003; Itoh et al. 1997; Ketterer et al. 1983; Kumagai et al. 2013; Toyama et al. 2011), whereas RSS produced by CSE can inactivate electrophiles through the sulfur adduct formation (Abiko et al. 2015a, 2015b, 2017a). These findings further support the presence of noncanonical pathway that detoxifies environmental electrophiles under the regulation of CSE, in addition to the canonical pathway regulated by Nrf2.

It is well recognized that Nrf2 plays a critical role in protection against oxidative and/or electrophilic stresses. In addition, Nrf2 regulates the metabolic homeostasis through regulating a number of detoxifying genes, such as *GCL*, *GST* (Itoh et al. 1997; Kim et al. 2010), and *MRP* (Hayashi et al. 2003), and glycogen- and glucose-metabolism genes, such as glycogen branching enzyme (*GBE*) and phosphorylase b kinase subunit (*PhK*) (Uruno et al. 2016). In agreement with other studies, we found that Nrf2 deletion increased sensitivity to environmental electrophiles MeHg (Toyama et al. 2007, 2011); Cd (Shinkai et al. 2016); 1,2-NQ (Miura et al. 2011); and 1,4-NQ (this study). Surprisingly, crotonaldehyde- and acrylamide-induced cytotoxicity were not affected substantially by single deletion of Nrf2. One plausible explanation for the observation is that certain defense mechanisms independent of Nrf2 may function against these reactive electrophiles. In fact, it has been reported that NADPH-dependent reductases are involved in detoxification of reactive carbonyls in plants (Yamauchi et al. 2011), presumably by

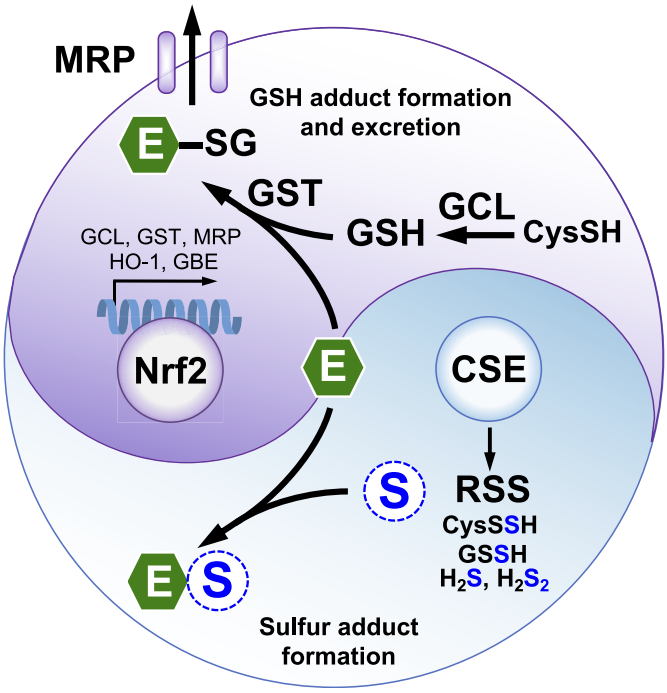

Figure 6. Schematic representation of parallel pathway in detoxifying environmental electrophiles. Transcription factor Nrf2 is a central coordinator for induction of detoxifying genes such as *GCL*, *GST*, *MRP*, and *HO-1* (Shen and Kong 2009; Yamamoto et al. 2018) and metabolic enzymes such as GBE (Uruno et al. 2016). Canonical pathway: Many *in vitro* and *in vivo* studies reported that Nrf2 contributes to detoxification of environmental electrophiles via GSH adduct formation and subsequent excretion into extracellular spaces (Miura et al. 2011; Toyama et al. 2007, 2011). Noncanonical pathway: Our mouse model provided that RSS generation mediated by CSE contributes to detoxifying environmental electrophiles through sulfur adduct formation. Note: CSE, cystathionine γ-lyase; E, environmental electrophile; GBE, glycogen branching enzyme; GCL, glutamate–cysteine ligase; GST, glutathione *S*-transferase; HO-1, hemeoxygenase-1; MRP, multidrug resistance-associated protein; Nrf2, nuclear factor-erythroid 2-related factor 2; RSS, reactive sulfur species.

reducing the carbonyl groups. Because expression levels of drug-metabolizing enzymes that catalyze carbonyl reduction are relatively high in hepatocytes (Agaton et al. 2003), Nrf2 may not be crucial to diminish carbonyl electrophile cytotoxicity.

In this regard, CSE is another critical factor for protection against electrophiles. CSE is involved in RSS production and thereby capturing electrophiles to yield their sulfur adducts (Abiko et al. 2015b; Millikin et al. 2016; Nishida et al. 2016; Ono et al. 2014; Yoshida et al. 2011). In fact, in the current study, we found that the cellular contents of CysSH, CysSSH, GSH, and GSSH were lower in CSE KO mice. Cd is an electrophilic metal responsible for causing acute hepatic injury *in vivo* (Rikans and Yamano 2000). We previously found that CSE deletion deteriorates Cd-induced hepatotoxicity (Akiyama et al. 2017; Shinkai et al. 2017). However, our current study revealed that CSE deletion did not affect substantially the cytotoxicity elicited by the other electrophiles; MeHg; 1,4-NQ; crotonaldehyde; and acrylamide in primary mouse hepatocytes. An explanation for this observation is that alternative defense pathway(s) may compensate the lack of CSE and protect cells from the electrophilic damage. Consistent with this notion, we found that CSE deletion enhanced Cd-mediated activation of Nrf2 and its downstream protein, HO-1. Such a phenomenon may be also seen in MeHg and 1,4-NQ because exposure of cultured cells to MeHg (Toyama et al. 2007; Unoki et al. 2018; Wang et al. 2009) and 1,4-NQ (Khan et al. 2011)-activated Nrf2

signaling pathway. We suggest that the function of Nrf2 is potentiated in CSE KO mice, thus protecting cells against electrophiles-mediated cell toxicity.

In contrast to the results *in vitro*, CSE deletion enhanced sensitivity to MeHg *in vivo*. It appears likely that such a difference between *in vitro* and *in vivo* in terms of MeHg toxicity is due to the transport system of MeHg into the brain. It is well-known that MeHg is converted to the MeHg–CysSH adduct to cross the blood–brain barrier (Kerper et al. 1992). We previously found that CSE deletion decreases production of $(MeHg)_2S$ after MeHg treatment (Abiko et al. 2015b), suggesting that formation and subsequent brain accumulation of the MeHg–CysSH adduct increases in the CSE KO mice.

DKO mice are highly sensitive to all environmental electrophiles examined *in vitro* and *in vivo*. Of note, crotonaldehyde- and acrylamide-induced cytotoxicity appeared not to be significantly affected by single deletion of Nrf2 or CSE, whereas compound deletion of Nrf2 and CSE markedly exacerbated the cytotoxicity caused by these carbonyl electrophiles. These results suggest that cellular defense mechanisms against these electrophiles are largely dependent on these two pathways, which can compensate for each other. Therefore, it appears that the detoxification ability mediated by Nrf2 or CSE is sufficient to block crotonaldehyde and acrylamide toxicity.

It has been shown that developing fetuses and neonates are highly susceptible to chemicals, including environmental electrophiles (Unüvar and Büyükgebiz 2012). For example, MeHg can easily pass through the placenta into the fetus via a neutral amino acid carrier, thereby causing adverse effects on fetal brain development (Onishchenko et al. 2007). Thus, the developing fetus and neonates are considered to be highly susceptible to MeHg in animals (Rice and Barone 2000) and humans (Grandjean et al. 1997, 2010; Knobeloch et al. 2007). Because the present study showed that deletion of CSE in mice exacerbated MeHg-induced neurological dysfunction, a lower level of CSE expression (Ishii et al. 2004) and its enzymatic activity, together with lower production of RSS at developmental stages, seem to cause the vulnerability to electrophiles. It is also known that there are sex differences in the vulnerability to electrophiles (Gandhi et al. 2014; Kim et al. 2014; Kippler et al. 2012; Shimada et al. 2012). Some studies have reported that the expression of RSS-producing enzymes, including CSE, is affected by sex hormones (Brancaleone et al. 2015; Vitvitsky et al. 2007). These findings lead us to speculate that CSE-dependent RSS level may potentially contribute to sex differences in the vulnerability to electrophiles. Since each experiment in this study employed either only one of male or female mice, we cannot exclude the possibility that the gender of the animal affected our results. Sex differences in the role of RSS in vulnerability to electrophiles should be investigated in the future study.

Although GSH is the most abundant sulfur nucleophile in various cells, it is largely protonated at physiological pH because of its high p*K*a value of approximately 9 (Armstrong 1991). For this reason, conjugation reactions of electrophiles with GSH are required because the p*K*a value decreases from 9 to 6–7 after the interaction of GSH with GST (Barry et al. 1995). However, p*K*a values of persulfides/polysulfides are lower than those of monosulfides, such as GSH and CysSH (Cuevasanta et al. 2015; Iciek et al. 2016). For example, the p*K*a value of CysSSH predicted by chemical calculations is estimated to be 4.34 (Cuevasanta et al. 2015), indicating that RSS are able to nonenzymatically react with environmental electrophiles to form their sulfur adducts at physiological pH, even without GST. Taken together, RSS-mediated protection against electrophiles appears to be a primary defense system compared with the Nrf2-dependent detoxification system with GSH, because RSS are constitutively produced by CSE and CARS2, whereas gene expression of GCL, GST, and MRP involved in conjugation with GSH and subsequent excretion of GSH adducts into extracellular space are cooperatively regulated by Nrf2 (Hayashi et al. 2003; Itoh et al. 1997). On the other hand, it is known that the expression of CSE is, at least in part, transcriptionally regulated by activating transcription factor 4 (ATF4) (Mistry et al. 2016; Sbodio et al. 2018). Some studies suggested that Nrf2 is a positive regulator of ATF4 under the condition of electrophilic stress (Afonyushkin et al. 2010; Terashima et al. 2013). Thus, cross talk between Nrf2 signaling and CSE expression might be mediated by ATF4 in response to environmental electrophile exposure.

While there are numerous reports of beneficial effects elicited by pretreatment with Nrf2 activators in food (e.g., vegetables, wine, and fruit) to repress toxicity (Iranshahy et al. 2018; Liu et al. 2016; Long et al. 2016; Noh et al. 2015) and cancer (Chen and Kong 2005; Talalay and Fahey 2001), we speculate that a direct trap of environmental electrophiles by intake of foods containing RSS would also be an effective strategy for electrophile detoxification. Therefore, we should focus on intake of food containing not only Nrf2 activators but also sulfane sulfur–dependent chemicals to diminish the health risks of environmental electrophiles.

Acknowledgments

This work was supported by Japan Society for the Promotion of Science Grants-in-Aid for Scientific Research (JSPS KAKENHI) Grant Numbers JP18H05293 to Y.K. and JP18K14895 to M.A. We thank M. Arico from Edanz Group (www.edanzediting.com/ac) for editing a draft of this manuscript.

References

Abiko Y, Ishii I, Kamata S, Tsuchiya Y, Watanabe Y, Ihara H, et al. 2015a. Formation of sulfur adducts of N-acetyl-p-benzoquinoneimine, an electrophilic metabolite of acetaminophen in vivo: participation of reactive persulfides. Chem Res Toxicol 28(9):1796–1802, PMID: 26304691, https://doi.org/10.1021/acs.chemrestox.5b00245.

Abiko Y, Sha L, Shinkai Y, Unoki T, Luong NC, Tsuchiya Y, et al. 2017a. 1,4-Naphthoquinone activates the HSP90/HSF1 pathway through the S-arylation of HSP90 in A431 cells: negative regulation of the redox signal transduction pathway by persulfides/polysulfides. Free Radical Bio Med 104:118–128, PMID: 28049024, https://doi.org/10.1016/j.freeradbiomed.2016.12.047.

Abiko Y, Shinkai Y, Unoki T, Hirose R, Uehara T, Kumagai Y. 2017b. Polysulfide Na2S4 regulates the activation of PTEN/Akt/CREB signaling and cytotoxicity mediated by 1,4-naphthoquinone through formation of sulfur adducts. Sci Rep 7(1):4814, PMID: 28684787, https://doi.org/10.1038/s41598-017-04590-z.

Abiko Y, Yoshida E, Ishii I, Fukuto JM, Akaike T, Kumagai Y. 2015b. Involvement of reactive persulfides in biological bismethylmercury sulfide formation. Chem Res Toxicol 28(6):1301–1306, PMID: 25874357, https://doi.org/10.1021/acs.chemrestox.5b00101.

Afonyushkin T, Oskolkova OV, Philippova M, Resink TJ, Erne P, Binder BR, et al. 2010. Oxidized phospholipids regulate expression of ATF4 and VEGF in endothelial cells via NRF2-dependent mechanism: novel point of convergence between electrophilic and unfolded protein stress pathways. Arterioscler Thromb Vasc Biol 30(5):1007–1013, PMID: 20185790, https://doi.org/10.1161/ATVBAHA.110.204354.

Agaton C, Galli J, Höidén Guthenberg I, Janzon L, Hansson M, Asplund A, et al. 2003. Affinity proteomics for systematic protein profiling of chromosome 21 gene products in human tissues. Mol Cell Proteomics 2(6):405–414, PMID: 12796447, https://doi.org/10.1074/mcp.M300022-MCP200.

Akaike T, Ida T, Wei FY, Nishida M, Kumagai Y, Alam MM, et al. 2017. Cysteinyl-tRNA synthetase governs cysteine polysulfidation and mitochondrial bioenergetics. Nat Commun 8(1):1177, PMID: 29079736, https://doi.org/10.1038/s41467-017-01311-y.

Akiyama M, Shinkai Y, Unoki T, Shim I, Ishii I, Kumagai Y. 2017. The capture of cadmium by reactive polysulfides attenuates cadmium-induced adaptive responses and hepatotoxicity. Chem Res Toxicol 30(12):2209–2217, PMID: 29116755, https://doi.org/10.1021/acs.chemrestox.7b00278.

Armstrong RN. 1991. Glutathione S-transferases: reaction mechanism, structure, and function. Chem Res Toxicol 4(2):131–140, PMID: 1782341, https://doi.org/10.1021/tx00020a001.

Barry TR, Waters P, Doonan S, Sheehan D. 1995. Structural investigation of a glutathione binding-site using computational analysis. Biochem Soc T 23(2):S382–S382, https://doi.org/10.1042/bst023382s.
Brancaleone V, Vellecco V, Matassa DS, d'Emmanuele di Villa Bianca R, Sorrentino R, Ianaro A , et al. 2015. Crucial role of androgen receptor in vascular H2S biosynthesis induced by testosterone. Br J Pharmacol 172(6):1505–1515, PMID: 24750035, https://doi.org/10.1111/bph.12740.
Chen C, Kong AN. 2005. Dietary cancer-chemopreventive compounds: from signaling and gene expression to pharmacological effects. Trends Pharmacol Sci 26(6):318–326, PMID: 15925707, https://doi.org/10.1016/j.tips.2005.04.004.
Cuevasanta E, Lange M, Bonanata J, Coitiño EL, Ferrer-Sueta G, Filipovic MR, et al. 2015. Reaction of hydrogen sulfide with disulfide and sulfenic acid to form the strongly nucleophilic persulfide. J Biol Chem 290(45):26866–26880, PMID: 26269587, https://doi.org/10.1074/jbc.M115.672816.
Delalande O, Desvaux H, Godat E, Valleix A, Junot C, Labarre J, et al. 2010. Cadmium-glutathione solution structures provide new insights into heavy metal detoxification. FEBS J 277(24):5086–5096, PMID: 21078121, https://doi.org/10.1111/j.1742-4658.2010.07913.x.
Denizot F, Lang R. 1986. Rapid colorimetric assay for cell-growth and survival. Modifications to the tetrazolium dye procedure giving improved sensitivity and reliability. J Immunol Methods 89(2):271–277, PMID: 3486233, https://doi.org/10.1016/0022-1759(86)90368-6.
Gandhi DN, Panchal GM, Dhull DK. 2014. Neurobehavioral toxicity in progeny of rat mothers exposed to methylmercury during gestation. Ann Ist Super Sanita 50(1):28–37, PMID: 24695250, https://doi.org/10.4415/ANN_14_01_05.
Gnedeva K, Hudspeth AJ. 2015. Soxc transcription factors are essential for the development of the inner ear. Proc Natl Acad Sci U S A 112(45):14066–14071, PMID: 26504244, https://doi.org/10.1073/pnas.1517371112.
Grandjean P, Satoh H, Murata K, Eto K. 2010. Adverse effects of methylmercury: environmental health research implications. Environ Health Perspect 118(8):1137–1145, PMID: 20529764, https://doi.org/10.1289/ehp.0901757.
Grandjean P, Weihe P, White RF, Debes F, Araki S, Yokoyama K, et al. 1997. Cognitive deficit in 7-year-old children with prenatal exposure to methylmercury. Neurotoxicol Teratol 19(6):417–428, PMID: 9392777, https://doi.org/10.1016/S0892-0362(97)00097-4.
Hayashi A, Suzuki H, Itoh K, Yamamoto M, Sugiyama Y. 2003. Transcription factor Nrf2 is required for the constitutive and inducible expression of multidrug resistance-associated protein 1 in mouse embryo fibroblasts. Biochem Biophys Res Commun 310(3):824–829, PMID: 14550278, https://doi.org/10.1016/j.bbrc.2003.09.086.
Iciek M, Kowalczyk-Pachel D, Bilska-Wilkosz A, Kwiecień I, Górny M, Wlodek L. 2016. S-sulfhydration as a cellular redox regulation. Biosci Rep 36(2):e00304, PMID: 26607972, https://doi.org/10.1042/BSR20150147.
Ida T, Sawa T, Ihara H, Tsuchiya Y, Watanabe Y, Kumagai Y, et al. 2014. Reactive cysteine persulfides and S-polythiolation regulate oxidative stress and redox signaling. P Natl Acad Sci USA 111(21):7606–7611, PMID: 24733942, https://doi.org/10.1073/pnas.1321232111.
Iranshahy M, Iranshahi M, Abtahi SR, Karimi G. 2018. The role of nuclear factor erythroid 2-related factor 2 in hepatoprotective activity of natural products: a review. Food Chem Toxicol 120:261–276, PMID: 30009889, https://doi.org/10.1016/j.fct.2018.07.024.
Ishii I, Akahoshi N, Yamada H, Nakano S, Izumi T, Suematsu M. 2010. Cystathionine gamma-lyase-deficient mice require dietary cysteine to protect against acute lethal myopathy and oxidative injury. J Biol Chem 285(34):26358–26368, PMID: 20566639, https://doi.org/10.1074/jbc.M110.147439.
Ishii I, Akahoshi N, Yu XN, Kobayashi Y, Namekata K, Komaki G, et al. 2004. Murine cystathionine gamma-lyase: complete cDNA and genomic sequences, promoter activity, tissue distribution and developmental expression. Biochem J 381(Pt 1):113–123, PMID: 15038791, https://doi.org/10.1042/BJ20040243.
Itoh K, Chiba T, Takahashi S, Ishii T, Igarashi K, Katoh Y, et al. 1997. An Nrf2 small Maf heterodimer mediates the induction of phase ii detoxifying enzyme genes through antioxidant response elements. Biochem Biophys Res Commun 236(2):313–322, PMID: 9240432, https://doi.org/10.1006/bbrc.1997.6943.
Jan AT, Azam M, Siddiqui K, Ali A, Choi I, Haq QM. 2015. Heavy metals and human health: mechanistic insight into toxicity and counter defense system of antioxidants. Int J Mol Sci 16(12):29592–29630, PMID: 26690422, https://doi.org/10.3390/ijms161226183.
Jiang YM, Wang Y, Tan HS, Yu T, Fan XM, Chen P, et al. 2016. Schisandrol B protects against acetaminophen-induced acute hepatotoxicity in mice via activation of the NRF2/ARE signaling pathway. Acta Pharmacol Sin 37(3):382–389, PMID: 26806302, https://doi.org/10.1038/aps.2015.120.
Kanda H, Shinkai Y, Kumagai Y. 2014. S-mercuration of cellular proteins by methylmercury and its toxicological implications. J Toxicol Sci 39(5):687–700, PMID: 25242398, https://doi.org/10.2131/jts.39.687.
Kaur P, Aschner M, Syversen T. 2006. Glutathione modulation influences methyl mercury induced neurotoxicity in primary cell cultures of neurons and astrocytes. Neurotoxicology 27(4):492–500, PMID: 16513172, https://doi.org/10.1016/j.neuro.2006.01.010.
Kerper LE, Ballatori N, Clarkson TW. 1992. Methylmercury transport across the blood-brain barrier by an amino acid carrier. Am J Physiol 262(5 Pt 2):R761–765, PMID: 1590471, https://doi.org/10.1152/ajpregu.1992.262.5.R761.
Ketterer B, Coles B, Meyer DJ. 1983. The role of glutathione in detoxication. Environ Health Perspect 49:59–69, PMID: 6339228, https://doi.org/10.1289/ehp.834959.
Khan NM, Sandur SK, Checker R, Sharma D, Poduval TB, Sainis KB. 2011. Pro-oxidants ameliorate radiation-induced apoptosis through activation of the calcium-ERK1/2-Nrf2 pathway. Free Radic Biol Med 51(1):115–128, PMID: 21530647, https://doi.org/10.1016/j.freeradbiomed.2011.03.037.
Kim J, Cha YN, Surh YJ. 2010. A protective role of nuclear factor-erythroid 2-related factor-2 (Nrf2) in inflammatory disorders. Mutat Res 690(1-2):12–23, PMID: 19799917, https://doi.org/10.1016/j.mrfmmm.2009.09.007.
Kim YD, Yim DH, Eom SY, Moon SI, Park CH, Kim GB, et al. 2014. Differences in the susceptibility to cadmium-induced renal tubular damage and osteoporosis according to sex. Environ Toxicol Pharmacol 38(1):272–278, PMID: 24975448, https://doi.org/10.1016/j.etap.2014.06.002.
Kippler M, Tofail F, Gardner R, Rahman A, Hamadani JD, Bottai M, et al. 2012. Maternal cadmium exposure during pregnancy and size at birth: a prospective cohort study. Environ Health Perspect 120(2):284–289, PMID: 21862444, https://doi.org/10.1289/ehp.1103711.
Knobeloch L, Gliori G, Anderson H. 2007. Assessment of methylmercury exposure in Wisconsin. Environ Res 103(2):205–210, PMID: 16831413, https://doi.org/10.1016/j.envres.2006.05.012.
Kumagai Y, Abiko Y. 2017. Environmental electrophiles: protein adducts, modulation of redox signaling, and interaction with persulfides/polysulfides. Chem Res Toxicol 30(1):203–219, PMID: 27981839, https://doi.org/10.1021/acs.chemrestox.6b00326.
Kumagai Y, Kanda H, Shinkai Y, Toyama T. 2013. The role of the Keap1/Nrf2 pathway in the cellular response to methylmercury. Oxid Med Cell Longev 2013:848279, PMID: 23878621, https://doi.org/10.1155/2013/848279.
Kumagai Y, Shinkai Y, Miura T, Cho AK. 2012. The chemical biology of naphthoquinones and its environmental implications. Annu Rev Pharmacol Toxicol 52:221–247, PMID: 21942631, https://doi.org/10.1146/annurev-pharmtox-010611-134517.
Kyhseandersen J. 1984. Electroblotting of multiple gels - a simple apparatus without buffer tank for rapid transfer of proteins from polyacrylamide to nitrocellulose. J Biochem Bioph Meth 10:203–209, PMID: 6530509, https://doi.org/10.1016/0165-022X(84)90040-X.
Li JJ, Li Q, Du HP, Wang YL, You SJ, Wang F, et al. 2015. Homocysteine triggers inflammatory responses in macrophages through inhibiting CSE-H2S signaling via DNA hypermethylation of CSE promoter. Int J Mol Sci 16(6):12560–12577, PMID: 26047341, https://doi.org/10.3390/ijms160612560.
Liu W, Xu C, Sun X, Kuang H, Kuang X, Zou W, et al. 2016. Grape seed proanthocyanidin extract protects against perfluorooctanoic acid-induced hepatotoxicity by attenuating inflammatory response, oxidative stress and apoptosis in mice. Toxicol Res (Camb) 5(1):224–234, PMID: 30090339, https://doi.org/10.1039/c5tx00260e.
Long M, Liu Y, Cao Y, Wang N, Dang M, He J. 2016. Proanthocyanidins attenuation of chronic lead-induced liver oxidative damage in kunming mice via the NRF2/ARE pathway. Nutrients 8(10):E656, PMID: 27775649, https://doi.org/10.3390/nu8100656.
Lu SC. 2013. Glutathione synthesis. Biochim Biophys Acta 1830(5):3143–3153, PMID: 22995213, https://doi.org/10.1016/j.bbagen.2012.09.008.
Millikin R, Bianco CL, White C, Saund SS, Henriquez S, Sosa V, et al. 2016. The chemical biology of protein hydropersulfides: Studies of a possible protective function of biological hydropersulfide generation. Free Radical Bio Med 97:136–147, PMID: 27242269, https://doi.org/10.1016/j.freeradbiomed.2016.05.013.
Mistry RK, Murray TV, Prysyazhna O, Martin D, Burgoyne JR, Santos C, et al. 2016. Transcriptional regulation of cystathionine-gamma-lyase in endothelial cells by NADPH oxidase 4-dependent signaling. J Biol Chem 291(4):1774–1788, PMID: 26620565, https://doi.org/10.1074/jbc.M115.685578.
Miura K, Clarkson TW. 1993. Reduced methylmercury accumulation in a methylmercury-resistant rat pheochromocytoma PC12 cell-line. Toxicol Appl Pharm 118(1):39–45, PMID: 8430423, https://doi.org/10.1006/taap.1993.1006.
Miura T, Shinkai Y, Jiang HY, Iwamoto N, Sumi D, Taguchi K, et al. 2011. Initial response and cellular protection through the Keap1/Nrf2 system during the exposure of primary mouse hepatocytes to 1,2-naphthoquinone. Chem Res Toxicol 24(4):559–567, PMID: 21384861, https://doi.org/10.1021/tx100427p.
Naganuma A, Oda-Urano N, Tanaka T, Imura N. 1988. Possible role of hepatic glutathione in transport of methylmercury into mouse kidney. Biochem Pharmacol 37(2):291–296, PMID: 3342085, https://doi.org/10.1016/0006-2952(88)90731-9.
Nishida M, Kumagai Y, Ihara H, Fujii S, Motohashi H, Akaike T. 2016. Redox signaling regulated by electrophiles and reactive sulfur species. J Clin Biochem Nutr 58(2):91–98, PMID: 27013774, https://doi.org/10.3164/jcbn.15-111.

Noh JR, Kim YH, Hwang JH, Choi DH, Kim KS, Oh WK, et al. 2015. Sulforaphane protects against acetaminophen-induced hepatotoxicity. Food Chem Toxicol 80:193–200, PMID: 25818464, https://doi.org/10.1016/j.fct.2015.03.020.

Onishchenko N, Tamm C, Vahter M, Hökfelt T, Johnson JA, Johnson DA, et al. 2007. Developmental exposure to methylmercury alters learning and induces depression-like behavior in male mice. Toxicol Sci 97(2):428–437, PMID: 17204583, https://doi.org/10.1093/toxsci/kfl199.

Ono K, Akaike T, Sawa T, Kumagai Y, Wink DA, Tantillo DJ, et al. 2014. Redox chemistry and chemical biology of H2S, hydropersulfides, and derived species: implications of their possible biological activity and utility. Free Radical Bio Med 77:82–94, https://doi.org/10.1016/j.freeradbiomed.2014.09.007.

Rice D, Barone S Jr. 2000. Critical periods of vulnerability for the developing nervous system: evidence from humans and animal models. Environ Health Perspect 108 Suppl 3(Suppl 3):511–533, PMID: 10852851, https://doi.org/10.1289/ehp.00108s3511.

Rikans LE, Yamano T. 2000. Mechanisms of cadmium-mediated acute hepatotoxicity. J Biochem Mol Toxicol 14(2):110–117, PMID: 10630425, https://doi.org/10.1002/(SICI)1099-0461(2000)14:2%3C110::AID-JBT7%3E3.0.CO;2-J.

Saeed M, Higginbotham S, Rogan E, Cavalieri E. 2007. Formation of depurinating N3adenine and N7guanine adducts after reaction of 1,2-naphthoquinone or enzyme-activated 1,2-dihydroxynaphthalene with DNA. Implications for the mechanism of tumor initiation by naphthalene. Chem Biol Interact 165(3):175–188, PMID: 17224140, https://doi.org/10.1016/j.cbi.2006.12.007.

Sbodio JI, Snyder SH, Paul BD. 2018. Golgi stress response reprograms cysteine metabolism to confer cytoprotection in Huntington's disease. Proc Natl Acad Sci U S A 115(4):780–785, PMID: 29317536, https://doi.org/10.1073/pnas.1717877115.

Shen G, Kong AN. 2009. Nrf2 plays an important role in coordinated regulation of Phase II drug metabolism enzymes and Phase III drug transporters. Biopharm Drug Dispos 30(7):345–355, PMID: 19725016, https://doi.org/10.1002/bdd.680.

Shimada H, Hashiguchi T, Yasutake A, Waalkes MP, Imamura Y. 2012. Sexual dimorphism of cadmium-induced toxicity in rats: involvement of sex hormones. Arch Toxicol 86(9):1475–1480, PMID: 22466070, https://doi.org/10.1007/s00204-012-0844-0.

Shinkai Y, Kimura T, Itagaki A, Yamamoto C, Taguchi K, Yamamoto M, et al. 2016. Partial contribution of the Keap1-Nrf2 system to cadmium-mediated metallothionein expression in vascular endothelial cells. Toxicol Appl Pharmacol 295:37–46, PMID: 26827822, https://doi.org/10.1016/j.taap.2016.01.020.

Shinkai Y, Masuda A, Akiyama M, Xian M, Kumagai Y. 2017. Cadmium-mediated activation of the HSP90/HSF1 pathway regulated by reactive persulfides/polysulfides. Toxicol Sci 156(2):412–421, PMID: 28115653, https://doi.org/10.1093/toxsci/kfw268.

Shinkai Y, Sumi D, Toyama T, Kaji T, Kumagai Y. 2009. Role of aquaporin 9 in cellular accumulation of arsenic and its cytotoxicity in primary mouse hepatocytes. Toxicol Appl Pharmacol 237(2):232–236, PMID: 19341753, https://doi.org/10.1016/j.taap.2009.03.014.

Steegborn C, Clausen T, Sondermann P, Jacob U, Worbs M, Marinkovic S, et al. 1999. Kinetics and inhibition of recombinant human cystathionine gamma-lyase. Toward the rational control of transsulfuration. J Biol Chem 274(18):12675–12684, PMID: 10212249, https://doi.org/10.1074/jbc.274.18.12675.

Sumi D. 2008. Biological effects of and responses to exposure to electrophilic environmental chemicals. J Health Sci 54(3):267–272, https://doi.org/10.1248/jhs.54.267.

Talalay P, Fahey JW. 2001. Phytochemicals from cruciferous plants protect against cancer by modulating carcinogen metabolism. J Nutr 131(11 Suppl):3027S–3033S, PMID: 11694642, https://doi.org/10.1093/jn/131.11.3027S.

Terashima J, Tachikawa C, Kudo K, Habano W, Ozawa S. 2013. An aryl hydrocarbon receptor induces VEGF expression through ATF4 under glucose deprivation in HepG2. BMC Mol Biol 14:27, PMID: 24330582, https://doi.org/10.1186/1471-2199-14-27.

Toyama T, Shinkai Y, Yasutake A, Uchida K, Yamamoto M, Kumagai Y. 2011. Isothiocyanates reduce mercury accumulation via an Nrf2-dependent mechanism during exposure of mice to methylmercury. Environ Health Persp 119(8):1117–1122, PMID: 21382770, https://doi.org/10.1289/ehp.1003123.

Toyama T, Sumi D, Shinkai Y, Yasutake A, Taguchi K, Tong KI, et al. 2007. Cytoprotective role of nrf2/keap1 system in methylmercury toxicity. Biochem Biophys Res Commun 363(3):645–650, PMID: 17904103, https://doi.org/10.1016/j.bbrc.2007.09.017.

Unoki T, Abiko Y, Toyama T, Uehara T, Tsuboi K, Nishida M, et al. 2016. Methylmercury, an environmental electrophile capable of activation and disruption of the Akt/CREB/Bcl-2 signal transduction pathway in SH-SY5Y cells. Sci Rep 6:28944, PMID: 27357941, https://doi.org/10.1038/srep28944.

Unoki T, Akiyama M, Kumagai Y, Goncalves FM, Farina M, da Rocha JBT, et al. 2018. Molecular pathways associated with methylmercury-induced Nrf2 modulation. Front Genet 9:373, PMID: 30271424, https://doi.org/10.3389/fgene.2018.00373.

Unüvar T, Büyükgebiz A. 2012. Fetal and neonatal endocrine disruptors. J Clin Res Pediatr Endocrinol 4(2):51–60, PMID: 22672860, https://doi.org/10.4274/jcrpe.569.

Uruno A, Yagishita Y, Katsuoka F, Kitajima Y, Nunomiya A, Nagatomi R, et al. 2016. Nrf2-mediated regulation of skeletal muscle glycogen metabolism. Mol Cell Biol 36(11):1655–1672, PMID: 27044864, https://doi.org/10.1128/MCB.01095-15.

Vitvitsky V, Prudova A, Stabler S, Dayal S, Lentz SR, Banerjee R. 2007. Testosterone regulation of renal cystathionine beta-synthase: implications for sex-dependent differences in plasma homocysteine levels. Am J Physiol Renal Physiol 293(2):F594–600, PMID: 17537983, https://doi.org/10.1152/ajprenal.00171.2007.

Wang L, Jiang H, Yin Z, Aschner M, Cai J. 2009. Methylmercury toxicity and Nrf2-dependent detoxification in astrocytes. Toxicol Sci 107(1):135–143, PMID: 18815141, https://doi.org/10.1093/toxsci/kfn201.

Yamamoto M, Kensler TW, Motohashi H. 2018. The KEAP1-NRF2 system: a thiol-based sensor-effector apparatus for maintaining redox homeostasis. Physiol Rev 98(3):1169–1203, PMID: 29717933, https://doi.org/10.1152/physrev.00023.2017.

Yamauchi Y, Hasegawa A, Taninaka A, Mizutani M, Sugimoto Y. 2011. NADPH-dependent reductases involved in the detoxification of reactive carbonyls in plants. J Biol Chem 286(9):6999–7009, PMID: 21169366, https://doi.org/10.1074/jbc.M110.202226.

Yoshida E, Toyama T, Shinkai Y, Sawa T, Akaike T, Kumagai Y. 2011. Detoxification of methylmercury by hydrogen sulfide-producing enzyme in mammalian cells. Chem Res Toxicol 24(10):1633–1635, PMID: 21951228, https://doi.org/10.1021/tx200394g.